

The Investigation of Ion Implantation as a Technique for Manufacturing GaAs Magneto-Sensitive Detectors

G F Karlova¹ and B I Avdochenko²

¹Leading Researcher at NIIPP, JSC, Tomsk, Russia

²Professor at TUSUR, Tomsk, Russia

E-mail: karlovagf@yandex.ru

Abstract. This paper studies thin active layers of n - n_i and n^+ - n - n_i -types produced by means of silicon ion implantation into a semi-insulating GaAs substrate. The results of these structures' physical parameters investigation are presented. Based on the structures the Hall-effect sensors are designed that have the linearity of Hall voltage dependency on magnetic density $U_H(B)$ of at least 1% in the range of up to $B < 1.2$ T.

1. Introduction

The interest of hardware engineers in sensitive and reliable magnetic-field detectors is dictated by both widespread development of automation and microelectronics and necessity of field density measurement. That is because detectors are the primary items for data acquisition from the object under measurement. The sensor operating threshold is determined by the ratio of the Hall-effect sensor probes voltage in the absence of magnetic field U_{res} to the output voltage in the presence of magnetic field U_H . In [1], the GaAs magnetic field detector based on epitaxial structure has been designed. The further step is to develop the magnetically controlled integrated circuit based on Schottky-barrier FETs. This represents a great challenge as the material with submicron thickness is required to create such devices. Furthermore, the net cost of epitaxial structures is relatively high. The ion implantation technique enables overcoming these difficulties and producing submicron structures for Hall-effect sensors.

This paper describes the technique for producing ion-doped GaAs structures, and reports the results of physical parameters investigation for these structures and Hall-effect sensors based on them.

2. Structure manufacturing technique

In the course of the research, the two types of structures have been obtained. They are n - n_i and n^+ - n - n_i , where n is a carrier density in active layer, n^+ is a carrier density in contact layer, and n_i is a carrier density in a substrate. Silicon doping was carried out by means of the installation "Vezuvy-5". Semi-insulating undoped GaAs substrate had the orientation of (100) and specific electrical resistance of more than 10^7 Ohm · cm. Post-implantation annealing was conducted in arsenic atmosphere at the temperature of 1123 K.

The preliminary estimation of the doped Si ion concentration profiles is conducted using the Gaussian distribution [20]:

$$N(x) = (D / (2\pi)^{1/2} \cdot \Delta R_p) \cdot \exp[-(x-R_p)^2 / 2 \cdot \Delta R_p^2], \quad (1)$$

where D is an ion-implantation dosage; x is a current position; R_p is a projective range for ions, ΔR_p is an rms deviation of the range for ions (what is called straggling). The range and the straggling were determined by means of Lindhard-Scharff-Schiott theory [2]. To find experimental dependencies of distribution profiles on different implantation parameters, the measurements were conducted under the



following conditions: a set of electron energies of 20–130 keV at the dosage of $3.75 \cdot 10^{12} \text{ cm}^{-2}$; a set of implantations dosages of $2.5 \cdot 10^{12}$ – $2 \cdot 10^{13} \text{ cm}^{-2}$ at the electron energy of 130 keV; and the dual implantation.

For produced layers several measurements of carrier density profile and mobility (μ) were conducted: measurement by Van-der-Pauw method with layer-by-layer etching under the room temperature; measurement by means of the profilometer EDK-6817 with mercury probe of small diameter; temperature measurement in the range of 85–400 K.

3. Key experimental results

1. The structures obtained have the following parameters: the structures of the first type — carrier density $n = (1.3\text{--}3.5) \cdot 10^{17} \text{ cm}^{-3}$, layer thickness $d = 250\text{--}340 \text{ nm}$, carrier mobility $\mu = 3000\text{--}3500 \text{ cm}^2/\text{V}\cdot\text{s}$, layer resistance $r = 600\text{--}650 \Omega/\text{sq}$; the structures of the second type — $n^+ = (1\text{--}2) \cdot 10^{18} \text{ cm}^{-3}$, $d = 70\text{--}80 \text{ nm}$, $n = (1.3\text{--}3) \cdot 10^{17} \text{ cm}^{-3}$, $d = 250\text{--}300 \text{ nm}$, $\mu = 2600\text{--}3200 \text{ cm}^2/\text{V}\cdot\text{s}$, $r = 400 \Omega/\text{sq}$.

2. The parameters of Hall-effect sensor (input and output resistance R_{in} and R_{out} , sensitivity γ , residual voltage U_{res} , operating current I) are dependent on Si ion implantation mode (the energy and the dosage), presence of n^+ -layer, and condition of the interface between the n -layer and the substrate. These data are shown in the following table.

Table 1. Types and parameters of the structures.

#	Type	$n, \text{ cm}^{-3}$	$R_{\text{in}}, \text{ k}\Omega$	$R_{\text{out}}, \text{ k}\Omega$	$I_{\text{max}}, \text{ mA}$	$U_{\text{res}}, \text{ mV}$	$\gamma, \text{ V/A}\cdot\text{T}$
1	$n\text{--}n_I$	$2.0 \cdot 10^{17}$	4	4	1.5	30–50	600–800
2	$n\text{--}n_I$	$3.0 \cdot 10^{17}$	1.75	1.8	10	1–3	200
3	$n\text{--}n_I$	$2.5 \cdot 10^{17}$	1.5–3	1.5–3	7	32–45	400
4	$n^+\text{--}n\text{--}n_I$	$2.0 \cdot 10^{17}$ ($n^+ = 1 \cdot 10^{18}$)	1.5–3	1.6–3	8	4–12	400
5	$n^+\text{--}n\text{--}n_I$	$3.5 \cdot 10^{17}$ ($n^+ = 1.5 \cdot 10^{18}$)	1.3–2	1.3–2	10	1–4	300–400

3. With the growth of density in n -layer, thickness of a space-charge region driven by surface potential gets lower. This leads to decrease of input resistance R_{in} , widening of operating current range, and reduction of residual voltage U_{res} and sensitivity γ (see structures 2 and 3 in Table 1).

4. The presence of n^+ -layer in Hall-effect sensor structure results in contact resistance drop and screening the surface potential off. In general, it improves Hall-effect sensor parameters (see structures 4 and 5 in Table 1).

5. The presence of trapping sites at the $n\text{--}n_I$ interface results in Hall-effect sensor sensitivity decrease as exemplified by the analysis of the relaxation curves obtained for the produced structures by means of GRAN-6 system.

6. The ohmic contacts' resistance asymmetry makes the main contribution to the U_{res} value.

7. The saturation area that is seen in a current-voltage curve can be explained by a backward control through the substrate and the presence of traps at the active layer surface [3].

4. Discussion of the experimental results

Figure 1 shows the profiles of Si ions doped with the dosage D of $3.75 \cdot 10^{12} \text{ cm}^{-2}$ and the energy of 130 keV (the solid curve is the one calculated using (1); the dots represent distribution of the electrically active carrier density after annealing). The difference between experimental and calculated curves is explained by the diffusion of doped ions during the annealing at the temperature of 1123 K. From the dependency of layer density on temperature it can be seen that density stays constant and

equals to $1.5 \cdot 10^{12} \text{ cm}^{-2}$ up to 400 K. The variation of mobility with the temperature in the range of up to 160 K is explained by ionized impurity scattering. In the range of $T > 160 \text{ K}$, it is explained by acoustic phonon scattering. These dependencies agree with calculated temperature dependencies for GaAs presented in [3]. However, the absolute value of the mobility is lower and at the room temperature equals $3.5 \cdot 10^3 \text{ cm}^2/\text{V} \cdot \text{s}$. It points to the presence of significant number of impurities in GaAs layers obtained. To explore the influence of deep trapping sites at the interface between the thin layer and the substrate the samples under investigation were put into the reflection-type microwave resonator operating at the frequency of 38 GHz. The conductivity was estimated through the proportional change of microwave power reflected from the resonator. The measurement was performed alongside with the application of the illumination by a visible-spectrum LED to the side of thin layer (or substrate) and the bias to n^+-n or $n-n_i$ interfaces. The typical picture is shown in Figure 2.

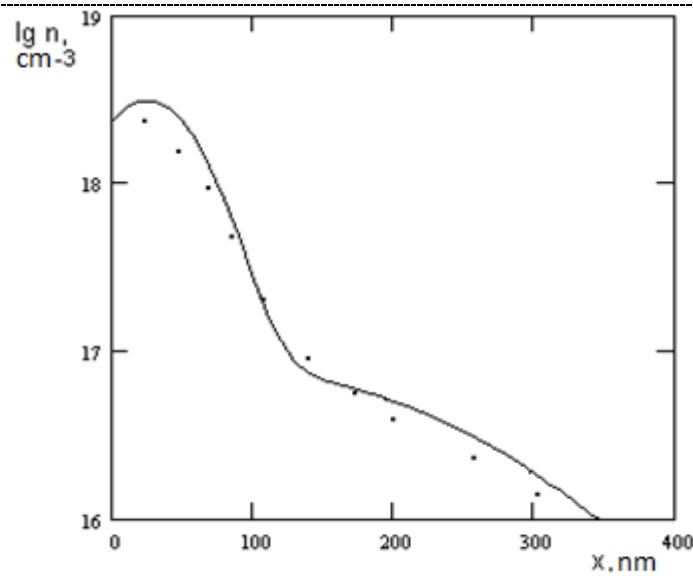


Figure 1. Distribution of carrier density across the depth (solid curve corresponds to calculated dependency, dots correspond to experimental data).

Figure 2 shows that the long-term relaxation of the light-induced conductivity comes from the recharge of deep level located inside the $n-n_i$ -junction. The recharge is resulted from the illumination (i. e. injection of holes into the $n-n_i$ -junction). For the samples under investigation, the charge carrier density profile in a bulk of epitaxial layer is estimated by means of voltage-capacitance curve obtained using the EDK 68-07 system. There is a peak at the interface between the thin layer and the substrate that can be explained by presence of deep trapping sites localized at the interface like in [4]. This

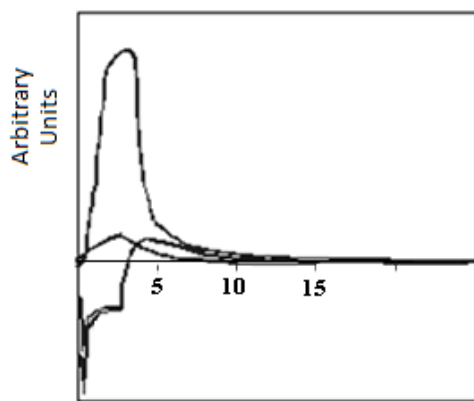


Figure 2. Photoresponse of the structure at different voltages under the forward (upper curves) and back (lower curves) biases.

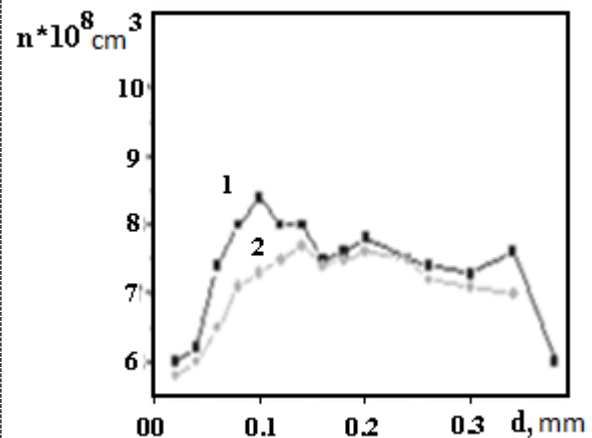


Figure 3. Distribution of carrier density across the depth depending on implantation parameters: curve 1 – 130 keV, $4 \cdot 10^{12} \text{ cm}^{-2}$; curve 2 – 130 keV, $3 \cdot 10^{12} \text{ cm}^{-2}$.

peak corresponds to the peak of light-induced conductivity when the reverse bias is applied to the structure (see Figure 2). The analysis of the relaxation conductivity curves for the interface between

the thin layer and the substrate shows that these defects can be explained by the quality of semi-insulating substrates.

The most important parameter of Hall-effect sensors is a residual voltage. It is associated with the resistance of planar ohmic contacts. For planar ohmic contacts with the length d_l and width w it can be found using the long line model [3]. The current I distribution under the contact with the length d is described by the following equation:

$$\frac{dI}{dx} = -J(x)w \quad (2),$$

where x is a position, w is a width of the contact, J is a current density that equals to

$$J(x) = \frac{U(x)}{r_{\text{ohm}}} \quad (3),$$

where r_{cont} is a contact reduced resistance [$\Omega \cdot \text{cm}^2$], $U(x)$ is a channel potential related to a metal contact.

$$\frac{dU(x)}{dx} = \frac{-I \cdot R_{\text{noe}}}{w} \quad (4),$$

where R_{surf} is a surface resistance [Ω/sq] of a semiconductive thin layer under the contact. The equations (1) and (3) resolve into the long line equation:

$$\frac{d^2U(x)}{dx^2} = \frac{U}{L_t} \quad (5),$$

where $L_t = (r_{\text{cont}}/R_{\text{surf}})^{1/2}$ is a so called attenuation distance.

The solution to the equation (5) in respect to sensors is presented in [5]. The expression for the residual voltage has the following form:

$$U_{\text{ocm}} = I_0 \cdot r_{\text{ohm}} \left(\text{ch} \frac{d}{L_t} \right)^{-1}. \quad (6)$$

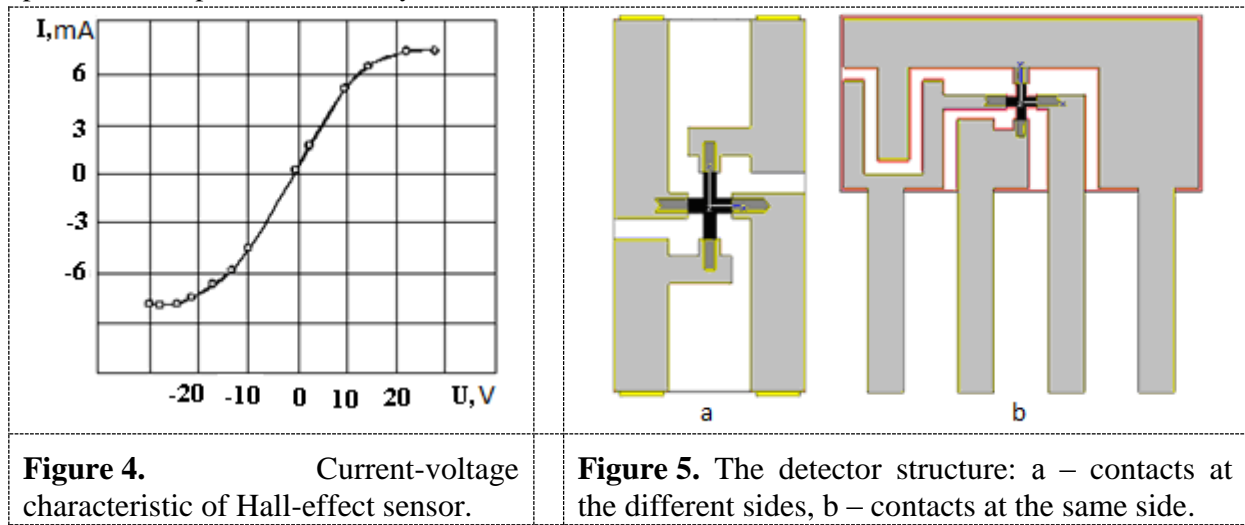
The r_{cont} and subsequently $U_{\text{res.k}}$ depend on depth of alloying. The value of contact resistance is defined both by the condition of the interface between alloyed and non-alloyed regions and by the condition of metal-semiconductor junction.

In the course of the research, investigations of r_{cont} dependency on evaporated contact alloying parameters (maximal annealing temperature, annealing time, annealing temperature gradient), epitaxial substrate surface treatment, and contact annealing atmosphere were conducted. Changes of contact alloying parameters and subsequent measurements of r_{cont} for tailored samples using Cox method [3] were carried out to obtain the dependency of r_{cont} on the maximal temperature with the minimum value shift depending on annealing atmosphere. In the hydrogen atmosphere the minimal reduced contact resistance was lower than the one in the nitrogen atmosphere. The reduced contact resistance is shown to be dependent on the carrier density in the active region, although the contact layer of all structures under investigation had low resistance. The minimal value of r_{cont} at the carrier density $n = 2 \cdot 10^{17} \text{ cm}^{-3}$ and $d = 0.4 \text{ um}$ is $4 \cdot 10^{-6} \Omega \cdot \text{cm}^2$ while $U_{\text{res}} = 0.4 \text{ mV}$, $U_{\text{H}} = 40 \text{ mV}$, and the ratio $U_{\text{res}}/U_{\text{H}} = 0.01$. The asymmetry of r_{cont} in sensor chips result in appearance of U_{res} in a magneto-sensitive detector.

It is also found out that the low residual voltage in Hall-effect sensor can be obtained only when the carrier density profile at the interface between the thin layer and the substrate is sharp. Figure 3 demonstrates concentration profiles for two implantation parameter sets (the curve 1: 130 keV, $4 \cdot 10^{12} \text{ cm}^{-2}$ and 50 keV, $5 \cdot 10^{12} \text{ cm}^{-2}$; the curve 2: 130 keV, $3 \cdot 10^{12} \text{ cm}^{-2}$ and 50 keV, $3 \cdot 10^{12} \text{ cm}^{-2}$). For the first parameter set the residual voltage value is no more than 0.1 mV.

The current-voltage characteristics for all samples under investigation were measured. All of them were linear in the range up to the value U_L that corresponds to the limiting current I_{lim} . At $U > U_L$ the current-voltage characteristic becomes saturated wherein the lower ($n \cdot d$) value, the earlier saturation

comes. This phenomenon can be explained by a backward control through the substrate, and the presence of traps at the active layer surface [3].



At the interface between the active layer and the substrate there is a charge-depletion layer of the definite thickness with the maximal width

$$d_{\max} \approx \left(\frac{1}{N_d} \ln \frac{N_d}{n_i} \right)^{\frac{1}{2}} \quad (7),$$

where N_d is a dopant density at the homogeneous doping, n_i is an intrinsic carrier density. In this case, the saturation current based on the model of field effect transistor without a gate [3] can be found using the following expression:

$$I_{\text{nac}} = N_d \cdot q \cdot A_{\text{act}} \cdot U_H \quad (8),$$

where A_{act} is a thickness of active region of a channel. The expressions (7) and (8) show that as the dopant density in the active region decreases, the value of d_{\max} increases and the saturation current gets lower.

The Hall-effect sensors are built on the obtained structures by means of the conventional GaAs technology used for manufacturing integrated circuits based on Schottky-barrier-gate FETs. Active region isolation of the magneto-sensitive detectors is performed by means of H, He and N ion doping. The Figure 5 shows the Hall-effect sensor structure. The die can be encapsulated in a compound or a SOT-8 package. In the first case, the total thickness will be no more than 1 mm, in the second one it will be 1.8 mm. The construction of the magneto-sensitive detector based on Hall-effect sensor with a ferrite ring helps to increase significantly the sensitivity of the current detectors designed today. The produced magneto-sensitive detectors have sensitivity $\gamma=200\text{--}560 \text{ V/A}\cdot\text{T}$. The dependencies of output voltage on magnetic density are linear and have nonlinearity factor no more than 1% at $B<1.2 \text{ T}$. The residual voltage for the structures with sharp profile is no more than $0.1 U_H$.

5. Conclusions

Based on the presented investigation, the following conclusions can be made:

1. The conducted estimation of carrier density profiles for ion doped structures is consistent with the experimental results obtained.
2. It is shown that to ensure low residual voltage carrier density profile at the interface between the thin layer and the substrate should be sharp.
3. The doped ions annealing parameters that ensure low r_{cont} are found. These parameters also ensure residual voltage value corresponding to the calculated one that is defined on the basis of the resistance of planar ohmic contacts.
4. The current-voltage curves of the structures obtained are linear only in a definite range, and then they go into saturation. The saturation can be explained by the backward control through the substrate, and the presence of traps at the active layer surface. The saturation current estimation agrees completely with the calculation.

The conducted investigation shows that it is possible to design Hall-effect sensors with high sensitivity ($\gamma \geq 560$ V/A T), low residual voltage ($U_{\text{res}} \leq U_{\text{H}}$), and nonlinearity factor of no more than 1% at $B < 1.2$ T by means of thin submicron layers ion implantation.

Acknowledgments

The research was conducted with financial support from the Ministry of Education and Science of the Russian Federation within the base part of the federal assignment № 2014/225 (project code 3643).

References

- [1] Karlova G, Porochovnichenko L and Umbras L Patent N2262777. 20.10.2005. *Bulletin* N29
- [2] Rissel X and Ruge I 1983 *Ion Implantation* (Moscow: Science)
- [3] Shur M 1991 *Modern devices based on gallium arsenide* (Moscow: World)
- [4] Karlova G, Porochovnichenko L The influence of interface between a thin layer and a substrate on the parameters of epitaxial semiconductor GaAs structures and Hall-effects sensors on their base. *Proceedings of the international conference "Physico-Chemical Processes in Inorganic Materials"* (Physical Chemical Problems-10), October 10–12 (2007) **2** 94–86
- [5] Karlova G F, Belopolova T J *Theses of the IXth Russian conference on semiconductor physics*. September 28 – October 3 (2009). Novosibirsk-Tomsk 332